Cell Reports

Article

Compartmentalized PGRP expression along the dipteran *Bactrocera dorsalis* gut forms a zone of protection for symbiotic bacteria

Graphical abstract

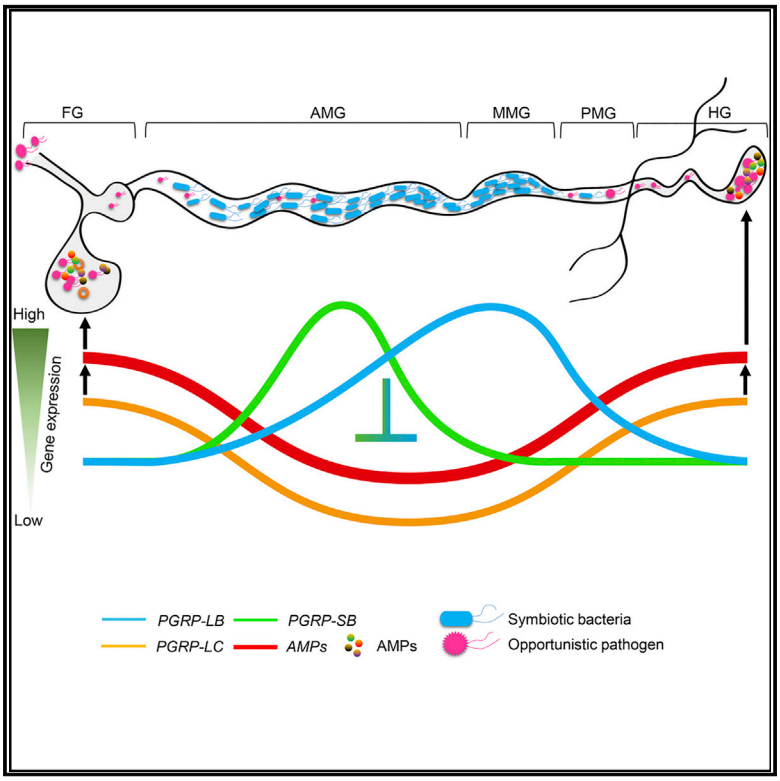

Authors

Zhichao Yao, Zhaohui Cai, Qiongke Ma, ..., Jian Gu, Bruno Lemaitre, Hongyu Zhang

Correspondence

hongyu.zhang@mail.hzau.edu.cn

In brief

Yao et al. find there is a regional expression of PGPR and spatial distribution of symbiotic bacteria along the *Bactrocera dorsalis* gut. This regional expression of PGPR tightly regulates the Imd pathway to construct a protective zone for symbiotic microbiota while maintaining the ability to fight pathogens.

Highlights

- Symbiotic bacteria are mainly located in the anterior midgut of *B. dorsalis*
- Regional expression of PGRP matches the distribution pattern of symbiotic bacteria
- *PGRP-LB* and *PGRP-SB* establish a protective zone for symbiotic bacteria colonization
- *PGRP-LC* and *AMPs* in the foregut filter the pathogens to protect symbiotic bacteria

Yao et al., 2022, Cell Reports *41*, 111523
October 18, 2022
https://doi.org/10.1016/j.celrep.2022.111523

CellPress

Cell Reports

CellPress
OPEN ACCESS

Article

Compartmentalized PGRP expression along the dipteran *Bactrocera dorsalis* gut forms a zone of protection for symbiotic bacteria

Zhichao Yao,[1] Zhaohui Cai,[1] Qiongke Ma,[1] Shuai Bai,[1] Yichen Wang,[1] Ping Zhang,[1] Qiongyu Guo,[1] Jian Gu,[1] Bruno Lemaitre,[2] and Hongyu Zhang[1,3,*]

[1]Key Laboratory of Horticultural Plant Biology (MOE), Hubei Hongshan Laboratory, Institute of Urban and Horticultural Entomology, College of Plant Science and Technology, Huazhong Agricultural University, Wuhan, People's Republic of China

[2]Global Health Institute, School of Life Science, École Polytechnique Fédérale de Lausanne (EPFL), Lausanne, Switzerland

[3]Lead contact

*Correspondence: hongyu.zhang@mail.hzau.edu.cn

https://doi.org/10.1016/j.celrep.2022.111523

SUMMARY

All metazoan guts are subject to opposing pressures wherein the immune system must eliminate pathogens while tolerating the presence of symbiotic microbiota. The Imd pathway is an essential defense against invading pathogens in insect guts, but tolerance mechanisms are less understood. Here, we find *PGRP-LB* and *PGRP-SB* express mainly in the anterior and middle midgut in a similar pattern to symbiotic Enterobacteriaceae bacteria along the *Bactrocera dorsalis* gut. Knockdown of *PGRP-LB* and *PGRP-SB* enhances the expression of antimicrobial peptide genes and reduces Enterobacteriaceae numbers while increasing abundance of opportunistic pathogens. Microbiota numbers recover to normal levels after the RNAi effect subsided. In contrast, high expression of *PGRP-LC* in the foregut allows increased antibacterial peptide production to efficiently filter the entry of pathogens, protecting the symbiotic bacteria. Our study describes a mechanism by which regional expression of PGRPs construct a protective zone for symbiotic microbiota while maintaining the ability to fight pathogens.

INTRODUCTION

The gut epithelium interacts with complex microbial communities that range from beneficial microorganisms to pathogens (Dillon and Dillon, 2004). Beneficial microorganisms influence host health and behavior in many ways, including provisioning of specific nutrients (Thong-On et al., 2012); protection from predators, parasites, and pathogens (Endt et al., 2010; Stecher and Hardt, 2011); and promotion of host growth and development (Shin et al., 2011). Alteration of intestinal microbiota composition, density, and function ("dysbiosis") has been associated with numerous host pathologies (Clark et al., 2015; Nyholm and Graf, 2012; Round and Mazmanian, 2009). Thus, maintaining gut microbiota homeostasis is essential for health of the host.

Gut microbiota may be affected by various environmental and host factors, such as food, age, pH range, and oxygen levels in the gut (Clark et al., 2015; Engel and Moran, 2013). Moreover, innate immunity is a key regulator of microbial abundance (Buchon et al., 2013b). Recent studies have shown two major immune pathways regulate gut microbiota homeostasis in insects. First is the production of microbicidal reactive oxygen species (ROS) by dual oxidase (Duox) and Nox (Iatsenko et al., 2018; Lee et al., 2013; Xiao et al., 2017; Yao et al., 2016). Second is the production of antimicrobial peptides (AMPs), regulated mainly by the immune deficiency (Imd) pathway (Broderick et al., 2014; Guo et al., 2013; Ryu et al., 2008). Duox-dependent ROS generation in the gut is dependent on the production of uracil by pathogenic but not commensal bacteria, allowing selective preservation of beneficial microbiota (Lee et al., 2013).

Studies in *Drosophila* have shown that the Imd pathway is activated upon the detection of diaminopimelic acid (DAP)-type peptidoglycan or peptidoglycan monomers, which are derived from nearly all gram-negative bacteria and some gram-positive bacteria, by the pattern recognition receptors PGRP-LC and PGRP-LE (Bosco-Drayon et al., 2012; Buchon et al., 2013b; Neyen et al., 2012). PGRP-LC is a transmembrane pattern recognition receptor that senses extracellular peptidoglycans, while PGRP-LE is an intracellular receptor thought to recognize cytoplasmic peptidoglycans. Both of these receptors recruit the Imd adaptor, converging to activate the transcription factor Relish (Buchon et al., 2013b). This pathway regulates the expression of antimicrobial peptides that can combat pathogens and shape microbiota composition (Liehl et al., 2006; Marra et al., 2021). Several mechanisms have been identified that keep the Imd pathway in check in the gut. Imd activity stimulates expression of amidase peptidoglycan recognition proteins (PGRPs) (such as PGRP-LB, PGRP-SB1, PGRP-SB2, PGRP-SC1a, PGRP-SC1b, and PGRP-SC2), which scavenge peptidoglycan and reduce its immunogenicity, establishing a negative

feedback loop that adjusts the magnitude of AMP production (Bischoff et al., 2006; Mellroth and Steiner, 2006; Zaidman-Rémy et al., 2006). Moreover, the transcription factor Caudal and the enzyme Transglutaminase dampen Imd pathway activation by repressing expression of nuclear factor kappa B-dependent antimicrobial peptides (Ryu et al., 2008; Shibata et al., 2013). Loss of several genes including *Caudal*, amidase PGRPs, and Transglutaminase disrupt gut microbiota homeostasis in *Drosophila* (Guo et al., 2013; Ryu et al., 2008; Shibata et al., 2013). However, the molecular mechanisms underlying the ability of the Imd pathway to accommodate the presence of beneficial microorganisms while mounting an effective immune response to combat pathogens is not fully established.

The Oriental fruit fly *Bactrocera dorsalis* (Hendel) (Diptera: Tephritidae) is a pest damaging more than 250 different species of fruits and vegetables worldwide. Its vast adaptability, high reproductive potential, and polyphagous nature make this insect one of the world's most invasive agricultural pests (Clarke et al., 2005; Li et al., 2011). In contrast to laboratory populations of *Drosophila*, in which the gut microbiota is transient and must be constantly replenished by ingestion to persist in most laboratory conditions (Broderick et al., 2014; Inês et al., 2018), *B. dorsalis* harbors a stable and complex bacterial community in which the dominant microbiota members belong to the family Enterobacteriaceae, and major genera include *Enterobacter*, *Citrobacter,* and *Klebsiella* (Wang et al., 2011, 2014). Previous studies have shown that these bacterial species were beneficial to their host insect *B. dorsalis* (Cai et al., 2018; Cheng et al., 2017; Li et al., 2020; Raza et al., 2020; Ren et al., 2021; Zhang et al., 2021). Therefore, *B. dorsalis* is emerging as an alternative insect model to decipher host-microbe interactions.

Using high-throughput sequencing and qPCR, we find that symbiotic bacteria are mainly located in the anterior midgut (AMG) of *B. dorsalis*, and their spatial distribution in different gut regions perfectly matches the expression profiles of *PGRP-LB* and *PGRP-SB,* two *PGRP* genes that negatively regulate the Imd pathway of *B. dorsalis*. Both *PGRP-LB* and *PGRP-SB* in the midgut restrain the host's immune response to provide a protective zone for symbiotic bacteria. Consistent with this, knockdown of *PGRP-LB* and *PGRP-SB* decreased the abundance of symbiotic bacteria in the AMG due to higher Imd pathway immune activation. In contrast, silencing the Imd pathway receptor gene *PGRP-LC,* which is expressed in the foregut, increases colonization by the opportunistic pathogen *P. rettgeri,* which ultimately overtakes the AMG and disrupts the microbiota. Our results clearly show that regional expression of pattern recognition receptor and amidase PGRPs tightly regulate the Imd pathway to tolerate symbiotic bacteria while barring colonization by pathogenic bacteria.

RESULTS

Symbiotic bacteria are mainly located in the anterior midgut of *B. dorsalis*

To clarify host mechanisms that regulate the gut microbiota, we used qPCR to investigate the distribution of bacteria along the *B. dorsalis* gut, which can be divided into three domains: foregut, midgut, and hindgut. Among them, the midgut can be further sub-divided into the anterior midgut (AMG), the middle midgut (MMG), and the posterior midgut (PMG) (Figures 1A and S1A). The density of Enterobacteriaceae and total bacteria was significantly higher in the AMG and MMG than in other gut regions (Figures 1B and 1C). Culture-dependent analysis of the gut microbiome corroborated these findings, indicating that colony-forming units (CFUs) of total culturable bacteria and culturable Enterobacteriaceae bacteria were both most abundant in the AMG (Figures 1D and 1E). More than 50% of CFUs in AMG and MMG were identified as *Citrobacter* and *Enterobacter* microbiota species (Figure 1F), with *Citrobacter koseri*, *Enterobacter cloacae*, and *Enterobacter hormaechei* being the dominant species (Table S1). The foregut had the richest bacterial community (comprising *Enterococcus*, *Lactococcus*, *Escherichia*, and *Arthrobacter* species, among others), while the opportunistic pathogens of the *Providencia* and *Morganella* genera were dominant in the PMG and hindgut (Figure 1F).

We next conducted high-throughput sequencing to more precisely define the community structure and the relative abundance of bacterial species residing in each gut region. The richness was highest in the foregut (90 unique OTUs per sample on average), then decreased to a stable level in following gut regions (Figure 1G). Based on Simpson diversity indexes, the AMG and MMG had the greatest diversity, and the hindgut had the lowest diversity (Figure 1G). Principal coordinate analyses (PcoA) revealed that the composition and structure of bacterial community varied with gut region, with PC1 and PC2 accounting for 76.71% and 15.24% of the observed variance, respectively (Figure 1H).

In terms of relative abundance, the high-throughput sequencing revealed that *Citrobacter*, *Enterobacter*, *Klebsiella*, *Serratia*, and other members of the Enterobacteriaceae dominated the AMG and MMG regions (Figure 1I). In the foregut, *Lactobacillus*, *Fructobacillus*, *Empedobacter, Comamonas, Dysgonomonas, Lactococcus, Vagococcus*, and *Sphingobacterium* bacteria were the dominant types; these gradually decreased to undetectable levels farther down the gut (Figure 1I). Opportunistic pathogens such as *Providencia* and *Morganella* bacteria were mainly present in the PMG region and hindgut (Figure 1I). Collectively, these results demonstrate that microbiota member distribution is regionalized along the gut. Bacteria that are known to be beneficial to the host are most abundant in the AMG and MMG regions, while few are present in the foregut and hindgut.

Regional activation of the Imd pathway inversely mirrors the distribution of symbiotic bacteria along the gut

To investigate potential impacts of host genes on the spatial distribution of symbiotic bacteria in the gut, we carried out transcriptomic sequencing of the five gut regions. Transcriptome assembly and annotation of immune-related genes identified a total of eight *AMPs* (*Attacin A*, *Attacin B*, *Attacin C*, *Diptericin*, *Phormicin*, *Sapecin*, *Cecropin*, and *Defensin*) and five genes encoding peptidoglycan-receptor proteins (*PGRP-LC*, *PGRP-LE*, *PGRP-LB*, *PGRP-SB*, and *PGRP-SC2*) expressed in the gut (Figures 2A–2D and S1B–S1D).

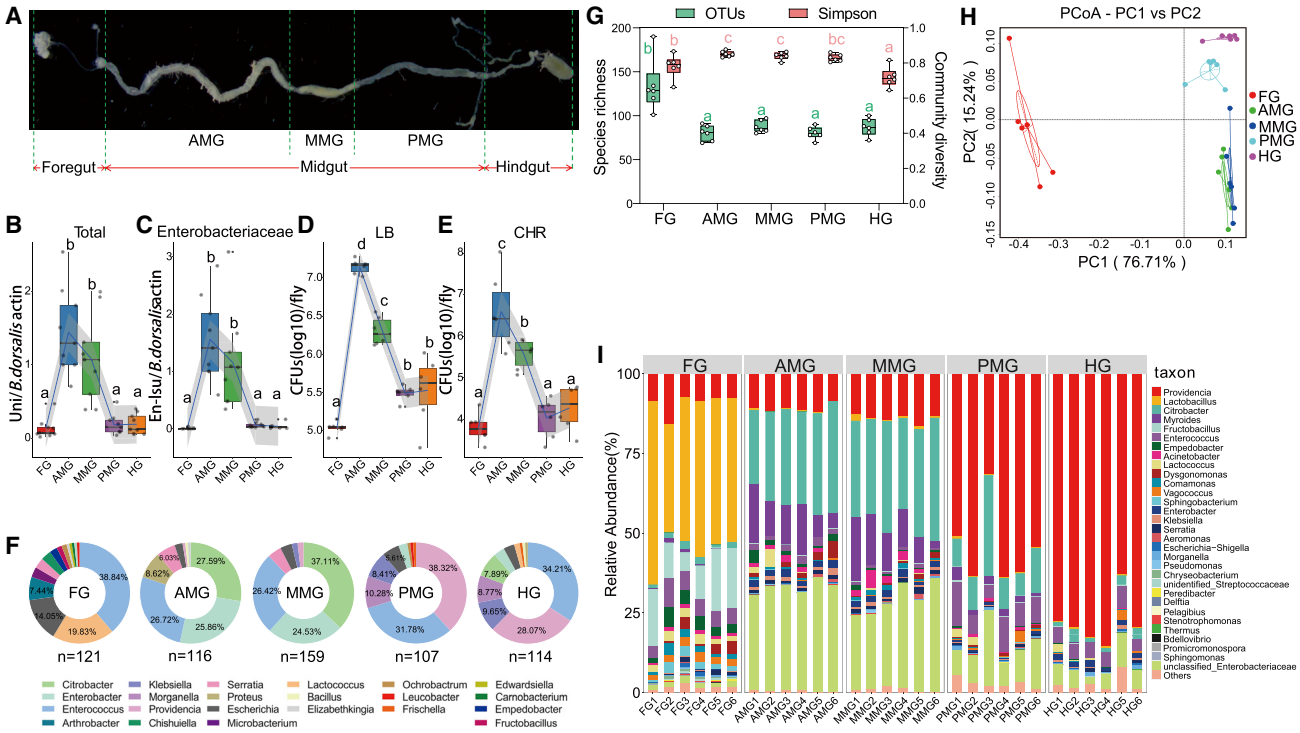

Figure 1. Morphology and distribution of symbiotic bacteria in different gut regions

(A) Morphology of the *B. dorsalis* gut from the pharynx to the rectum. The dotted lines indicate the borders between the different compartments.

(B and C) Total and Enterobacteriaceae bacterial density was assessed in the various gut regions using qPCR.

(D and E) Bacterial numbers in the indicated gut regions. CFUs of all culturable bacteria and symbiotic bacteria were quantified using selective plates: (D) Luria-Bertani agar (for all culturable bacteria); (E) CHROMagar Orientation medium (for symbiotic Enterobacteriaceae). The lower and upper limits of each box in (B–E) define the 25th and 75th percentiles, and the median is represented by the black lines; the dots represent biological replicates, n = 9 in (B and C), with a pool of 30 gut regions in each replicate; n = 6 in (D and E), with a pool of 25 gut regions in each replicate. Lines in (B–E) show median values per region window, and the shaded area denotes the estimated 95% confidence interval.

(F) The composition of culturable bacteria in different gut regions.

(G) Boxplot of species richness (number of OTUs, green box) and community diversity, measured using the Simpson index (pink box) (n = 6). Box-and-whisker plots show high, low, and median values, with the lower and upper edges of each box denoting first and third quartiles, respectively. Multiple comparisons in (B–E) and (G) were performed with one-way ANOVA (Tukey's post hoc test); different letters indicate significant differences between different gut regions at a p-value < 0.05.

(H) Principal coordinate analysis showing gut bacterial community structure based on Bray-Curtis dissimilarities. Each symbol represents a sample, colored by different gut regions.

(I) Relative genus-level abundance profiles of bacteria in different gut regions. Each bar in the plot represents a biological replicate (n = 6) with a pool of 100 gut regions each. AMG, anterior midgut; FG, foregut; HG, hindgut; MMG, middle midgut; PMG, posterior midgut. See also Figure S1.

We found that the membrane-bound *PGRP-LC* was highly expressed in the foregut and hindgut, while the intracellular receptor gene *PGRP-LE* was highly expressed in the AMG region (Figures 2A and 2C). This expression pattern of *PGRP-LC* in the gut of *B. dorsalis* is similar to that in *Drosophila* (Neyen et al., 2012). Consistent with the distribution pattern of *PGRP-LC*, six *AMP* genes (*Attacin A*, *Attacin B*, *Attacin C*, *Diptericin*, *Phormicin*, and *Sapecin*) were also expressed in the foregut and hindgut but were minimally expressed (if at all) in other gut regions (Figures 2B and 2D). We further confirmed regional activation of the Imd pathway along the *B. dorsalis* gut by monitoring the expression of *Diptericin*, an important effector gene of the Imd pathway, using fluorescence *in situ* hybridization (FISH). As expected, *Diptericin* expression was enriched in the foregut and the hindgut (Figure S1E). We did note that two other *AMP* genes, *Cecropin* and *Defensin*, were highly expressed in the AMG (Figures S1B–S1D). Different from *Attacins* and *Diptericin*, which are mostly regulated by the Imd pathway and primarily exhibit antibacterial activity (Hanson et al., 2019; Lemaitre and Hoffmann, 2007), *Cecropin* and *Defensin* are regulated by Imd, Toll, and other pathways, and have both antibacterial and some antifungal activities (Carboni et al., 2022; Hanson et al., 2019; Hedengren-Olcott et al., 2004; Pan et al., 2012; Tanji et al., 2010).

Importantly, Spearman correlation analysis showed that the expression profiles of *PGRP-LC* and *AMPs* are negatively correlated with the relative abundance and density of Enterobacteriaceae bacteria (including *Citrobacter*, *Klebsiella*, *Enterobacter*, *Serratia*, and Enterobacteriaceae_unclassified) (Figures 2F and 2G). Thus, the expression profile for *PGRP-LC* and the six immune effector genes that reflect Imd pathway activity inversely mirror the distribution of symbiotic bacteria in the

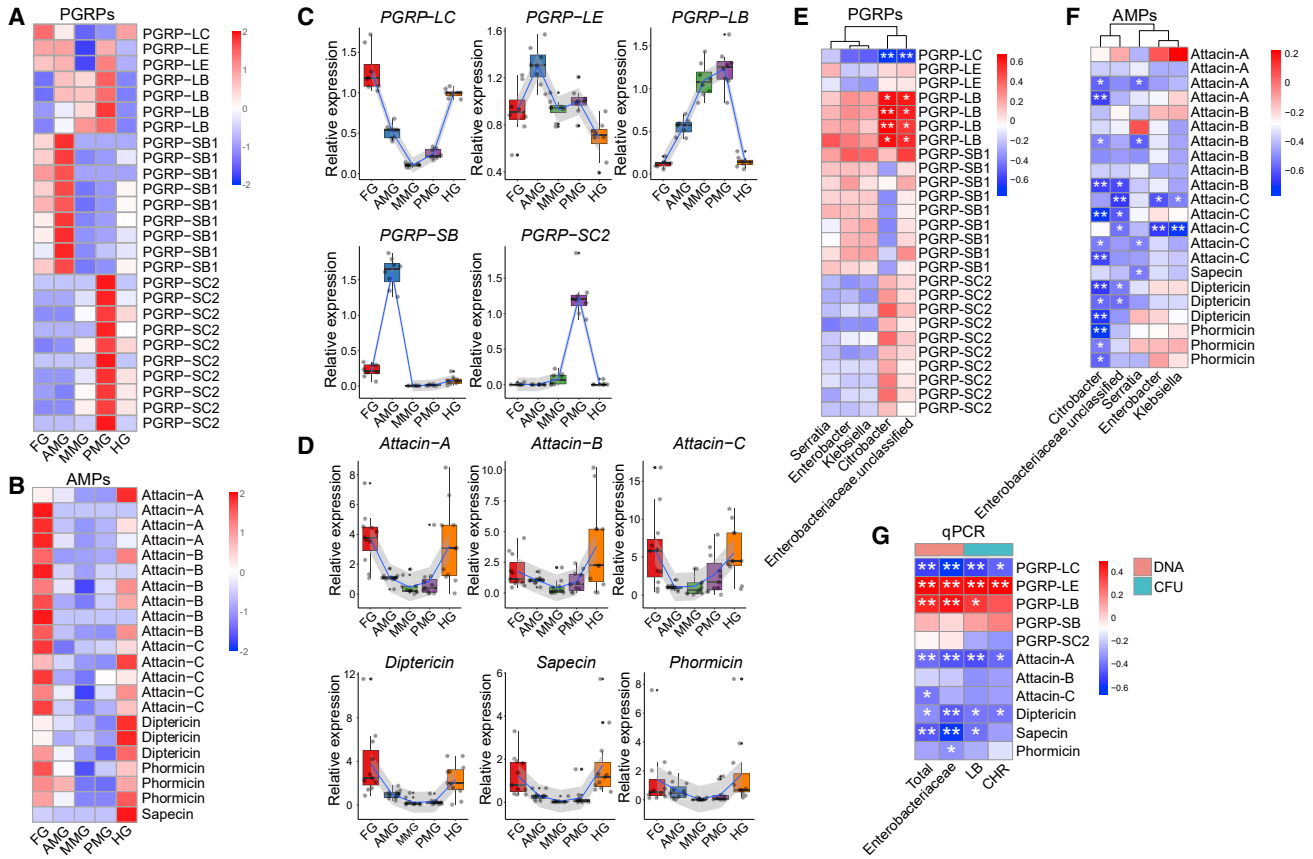

Figure 2. Expression profiling of Imd pathway genes and evaluation of potential spatial relationships with the distribution of symbiotic bacteria in various gut regions

(A and B) Heat map showing the relative expression levels of genes encoding PGRPs and *AMP* genes in the indicated *B. dorsalis* gut regions. The map is plotted based on Log2-transformed FPKM values, each bar or column corresponds to the relative gene expression level of gene in one gut region, with warmer colors representing higher relative gene expression levels.

(C and D) qPCR analysis of PGRPs and *AMP* gene expression in various gut regions. Box-and-whisker plots show high, low, and median values, with lower and upper edges of each box denoting the first and third quartiles, respectively. Lines in (C and D) show median values per region window, and the shaded area denotes the estimated 95% confidence interval. The dots represent biological replicates, n = 8 in (C), n = 11 in (D), with a pool of 30 gut regions in each replicate.

(E and F) Heatmaps of Spearman correlation between the relative abundance of Enterobacteriaceae bacteria and PGRPs (E) and *AMPs* (F).

(G) Spearman correlation analysis between the density of bacteria (including qPCR and $\log_{10}^{CFUs}$ data) and Imd pathway gene expression levels. Blue represents negative correlation between gene expression and bacterial genus or density, and red represents a positive correlation. *$p < 0.05$, **$p < 0.01$ with R statistical analysis by using cor.test. See also Figure S1.

midgut. This suggests that regional activity of the Imd pathway delineates zones suitable for the growth of beneficial bacteria.

Negative regulators of the Imd pathway match the distribution pattern of symbiotic bacteria along the gut

We then investigated the mechanism generating the pattern of Imd pathway activity along the digestive tract. Imd signaling is tightly controlled by multiple negative regulators, notably amidase PGRPs that can scavenge peptidoglycans (Bosco-Drayon et al., 2012; Bischoff et al., 2006; Mellroth and Steiner, 2006; Zaidman-Rémy et al., 2006). Interestingly, our RNA sequencing study reveals that three amidase PGRP genes, *PGRP-LB*, *PGRP-SB*, and *PGRP-SC2,* are expressed along the digestive tract. Further analysis of transcriptome and qPCR data showed that *PGRP-LB*, *PGRP-SB*, and *PGRP-SC2* were expressed in the midgut but not in the foregut or hindgut where Imd pathway activity is high (Figures 2A and 2C), revealing a pattern opposite to the expression of *PGRP-LC* and *AMPs* (Figures 2B and 2D). More specifically, *PGRP-LB* was highly expressed throughout all three midgut sub-regions, *PGRP-SB* was highly expressed in the AMG region, and *PGRP-SC2* was highly expressed in the PMG region (Figures 2A and 2C). Spearman correlation analysis showed that expression profiles of *PGRP-LB* and *PGRP-SB* are positively correlated with the relative abundance and density of Enterobacteriaceae bacteria in different gut regions (Figures 2E and 2G). These observations suggested that *PGRP-LB* and *PGRP-SB* but not *PGRP-SC2* (due to its restricted expression in PMG) could play a role in limiting Imd pathway activity in the AMG creating a zone favorable to symbiotic bacteria.

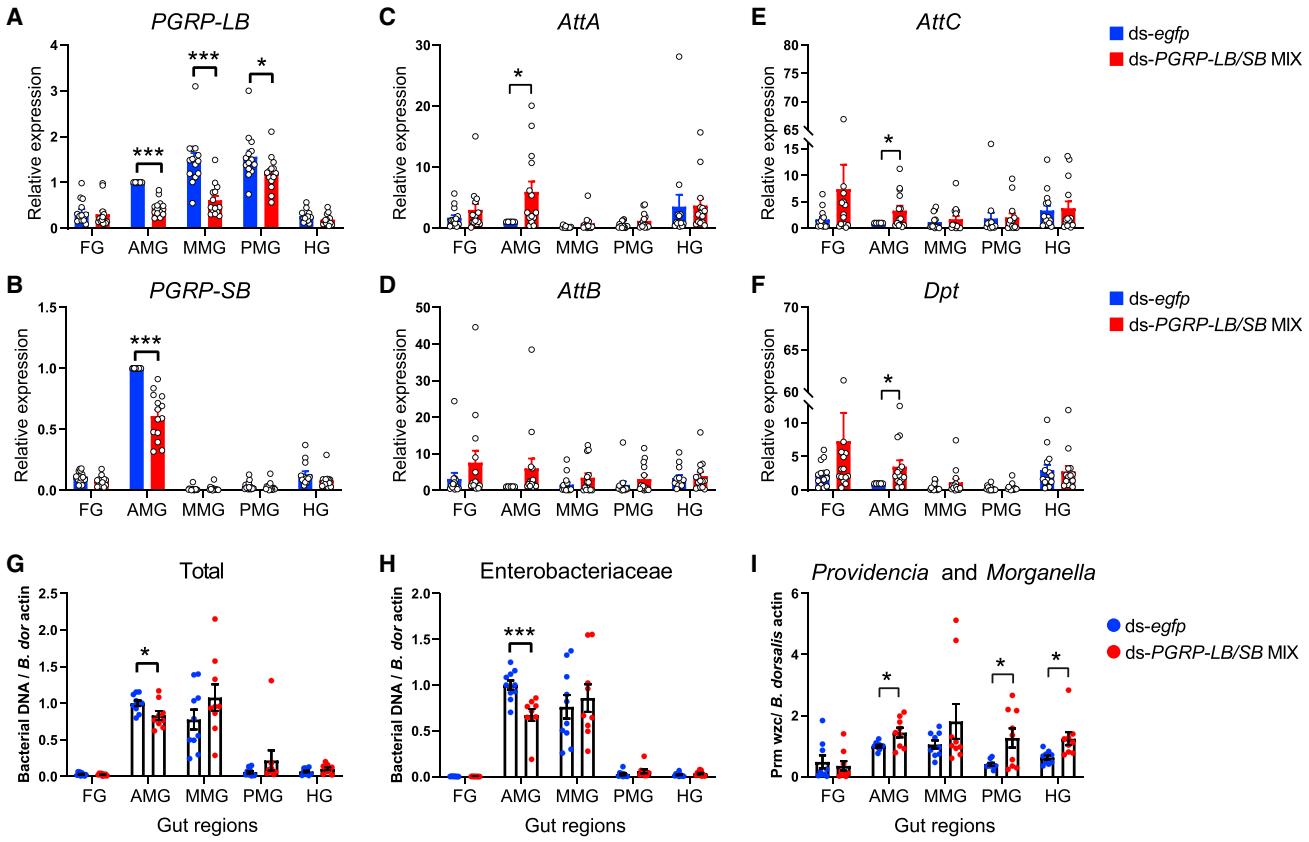

Figure 3. *B. dorsalis* lacking *PGRP-LB/SB* have an altered gut microbiota

(A and B) Quantification of *PGRP-LB* and *PGRP-SB* mRNA expression in different gut regions at 5 days post dsRNA injection (DPI).

(C–F) The Imd pathway activation was upregulated by *PGRP-LB/SB* knockdown. qPCR analysis of *AttA* (C), *AttB* (D), *AttC* (E), and *Dpt* (F) expression in different gut regions at 5 DPI (n = 14 biological replicates). For (A–F), values were normalized to *Rpl32* expression, mRNA levels in AMG were set to 1, and values obtained with other gut regions were expressed as a fold of this value.

(G–I) The compartmentalized microbial community homeostasis was disrupted by knockdown of *PGRP-LB/SB*. Total (G, n = 9–10), Enterobacteriaceae (H, n = 9–10), and *Providencia* and *Morganella* (I, n = 9) bacterial density were detected in different gut regions at 5 DPI by qPCR. Values were normalized to *β-actin* expression. Each dot represents a sample containing 30 gut regions. Data are represented as mean ± SEM, *p < 0.05, ***p < 0.001 with a two-tailed Student's t test. See also Figures S2 and S3.

Both *PGRP-LB* and *PGRP-SB* restrain immune effector expression in the midgut to establish protective zones for symbiotic bacteria

The results above prompted us to investigate the effects of Imd pathway activation on the distribution of gut microbiota by inducing double-stranded RNA (dsRNA) knockdown of the two pattern recognition receptor PGRPs that activate the Imd pathway, *PGRP-LC* and *PGRP-LE,* and the two negative regulator PGRPs, *PGRP-LB* and *PGRP-SB*, and monitoring impacts on the density of symbiotic bacteria using qPCR. We first showed that there was no off-target effect among *PGRP-LC*, *PGRP-LE*, *PGPR-LB*, and *PGPR-SB* knockdown experiment when silencing these genes in *B. dorsalis* (Figures S2A–S2D). Decreased *AMP* gene expression upon *PGRP-LC* or *PGRP-LE* knockdown did not affect total or Enterobacteriaceae bacterial density in any of the five gut regions (Figures S2E and S2F; Figures S2I–S2L). In addition, single knockdown of *PGRP-LB* or *PGRP-SB* had very mild effects on *AMP* gene expression, with a small increased the expression level of *Dpt* in ds-*PGRP-LB* or ds-*PGRP-SB* treated flies, a very slight increase of *AttA* expression in ds-*PGRP-SB* treated flies, while other *AMPs* were expressed at wild-type levels (Figures S2G and S2H). The minor impact on *AMP* gene expression might be the reason why knockdown of *PGPRP-LB* or *PGPR-SB* had no impact on the density of total or Enterobacteriaceae bacteria in each of the five gut regions (Figures S2M–S2P).

The lack of impact of *PGRP-LB* or *PGRP-SB* knockdown could be due to redundancy between these two amidase PGRPs. To test this notion, we injected flies with a mix of ds-*PGRP-LB* and ds-*PGRP-SB* and monitored *AMP* gene expression. Interestingly, simultaneous knockdown of these genes significantly enhanced the level of Imd pathway activity in the gut at 5 days post injection (DPI). Particularly, the expression of *AttA*, *AttC*, and *Dpt* was strongly increased in the AMG region, where both *PGRP-LB* and *PGRP-SB* are enriched, while no change in *AMP* expression was observed in other gut regions (Figures 3A–3F). Simultaneous knockdown of *PGRP-LB* and *PGRP-SB* also led to significant reductions in the total bacterial

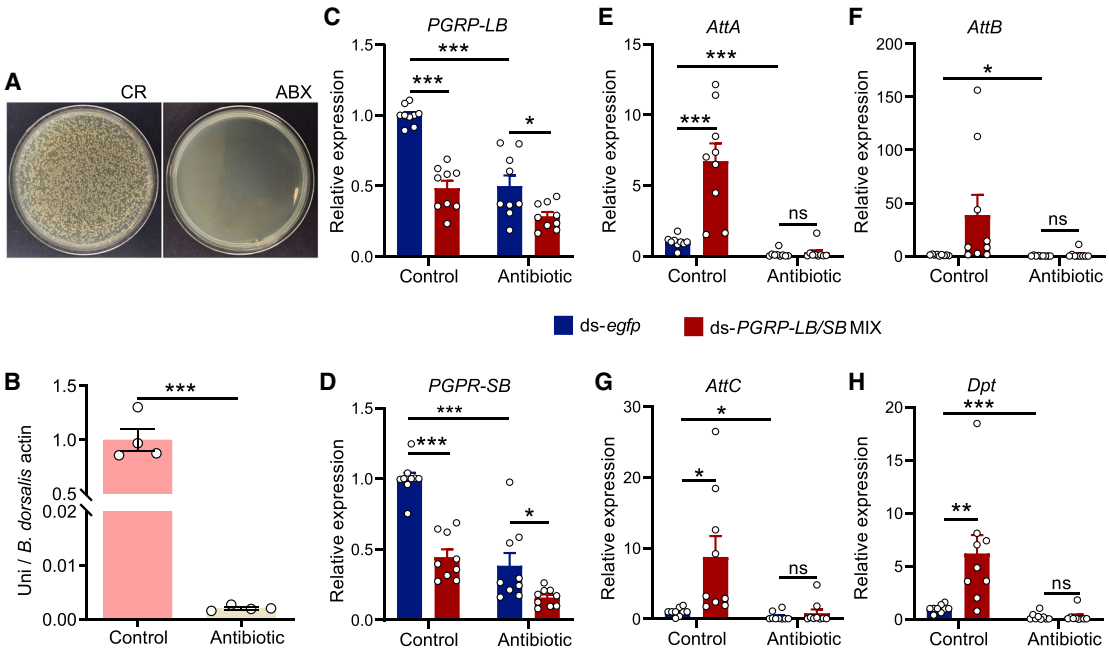

Figure 4. Overactivation of the Imd pathway induced by *PGRP-LB/SB* RNAi is symbiotic microbe-dependent

(A and B) The efficacy of elimination of gut bacteria verified by plating conventionally reared (CR) and antibiotic treated (ABX) flies' whole gut homogenates (10 guts per group) on LB agar plates (A), and performing qPCR analysis of total bacterial abundance by using universal gene primers (B, n = 4). Values were normalized to *β-actin* expression.

(C–H) RNAi knockdown of *PGRP-LB* (C) and *PGRP-SB* (D) in the AMG at 5 DPI was not influenced by the absence of gut commensal bacteria, but the absence of gut commensal bacteria abolished the overexpression of *AttA* (E), *AttB* (F), *AttC* (G), and *Dpt* (H) in the AMG induced by simultaneous knockdown of *PGRP-LB* and *PGRP-SB*. *PGRP-LB*, *PGRP-SB*, *AttA*, *AttB*, *AttC*, and *Dpt* expression in the AMG was measured with qPCR (n = 9). All values were normalized to *Rpl32* expression. Data represent mean ± SEM for biological replicates, *p < 0.05, **p < 0.01, ***p < 0.001 with a two-tailed Student's t test, ns, not significant (p > 0.05).

density, including Enterobacteriacae, in the AMG region, while no changes were observed in other gut regions (Figures 3G and 3H). This observation strongly suggests that higher *AMP* gene expression in the absence of negative regulators affects the maintenance of symbiotic bacteria. In addition, we observed a significant increase of the density of opportunistic pathogens such as *Providencia* and *Morganella* in the AMG, PMG, and HG regions of *PGRP-LB/SB* double-knockdown flies (Figure 3I).

We further monitored dynamic changes in *AMP* expression and bacterial community at 10 DPI when the RNAi effect on *PGRP-LB* and *PGRP-SB* was lost (Figures S3A and S3B). We found that the expression of *PGRP-LB* and *PGRP-SB* and AMP-encoding genes at 10 DPI returned to the same levels as controls (Figures S3C–S3H). Dysbiosis induced by double ds-*PGRP-LB/SB* knockdown similarly subsided at this late time point (Figures S3I–S3K). Altogether, our results demonstrate that two negative regulators of the Imd pathway, the amidase PGRPs *PGRP-LB* and *PGRP-SB,* generate a suitable zone in the AMG for enrichment of symbiotic Enterobacteriaceae bacteria in *B. dorsalis* gut by dampening *AMP* expression.

Symbiotic bacteria activate the expression of *PGRP-LB* and *PGRP-SB,* which dampens *AMP* expression in the AMG

To better understand the relationship between symbiotic bacteria and regulation of Imd pathway activity in the AMG, we analyzed the expression of *PGRP-LB*, *PGRP-SB*, and *AMP* genes in the gut of conventionally reared and antibiotic treated (ABX) flies (Figures 4A and 4B). Expression levels of *PGRP-LB*, *PGRP-SB*, *AttA*, *AttB*, *AttC*, and *Dpt* were significantly higher in conventional flies than in ABX-treated flies (Figures 4C–4H). Consistent with the above results, simultaneous knockdown of *PGRP-LB* and *PGRP-SB* induced the overexpression of *AMPs* in the AMG of conventional flies but not in ABX-reared flies (Figures 4E–4H). This suggests that symbiotic bacteria stimulate the Imd pathway, leading to the expression of the genes encoding *AMPs* and negative regulators of the Imd pathway, but that both *PGRP-LB* and *PGRP-SB* restrain activity of Imd pathway in the AMG to generate an environment favorable to beneficial bacteria.

Imd pathway activation in the foregut contributes to host defense against bacterial invasion

The results above show that *PGRP-LB* and *PGRP-SB* prevent overactivation of the Imd pathway in the AMG compartment where the microbiota reside. This raised the question of how the Imd pathway can still be activated to fight the entry of pathogenic bacteria. We noted that Imd pathway recognition receptor *PGRP-LC* and *AMPs* are expressed at a higher level in the foregut, suggesting that one of the main functions of the Imd pathway in the foregut could be to eliminate invading microbes. To explore this, we fed flies with the opportunistic pathogen

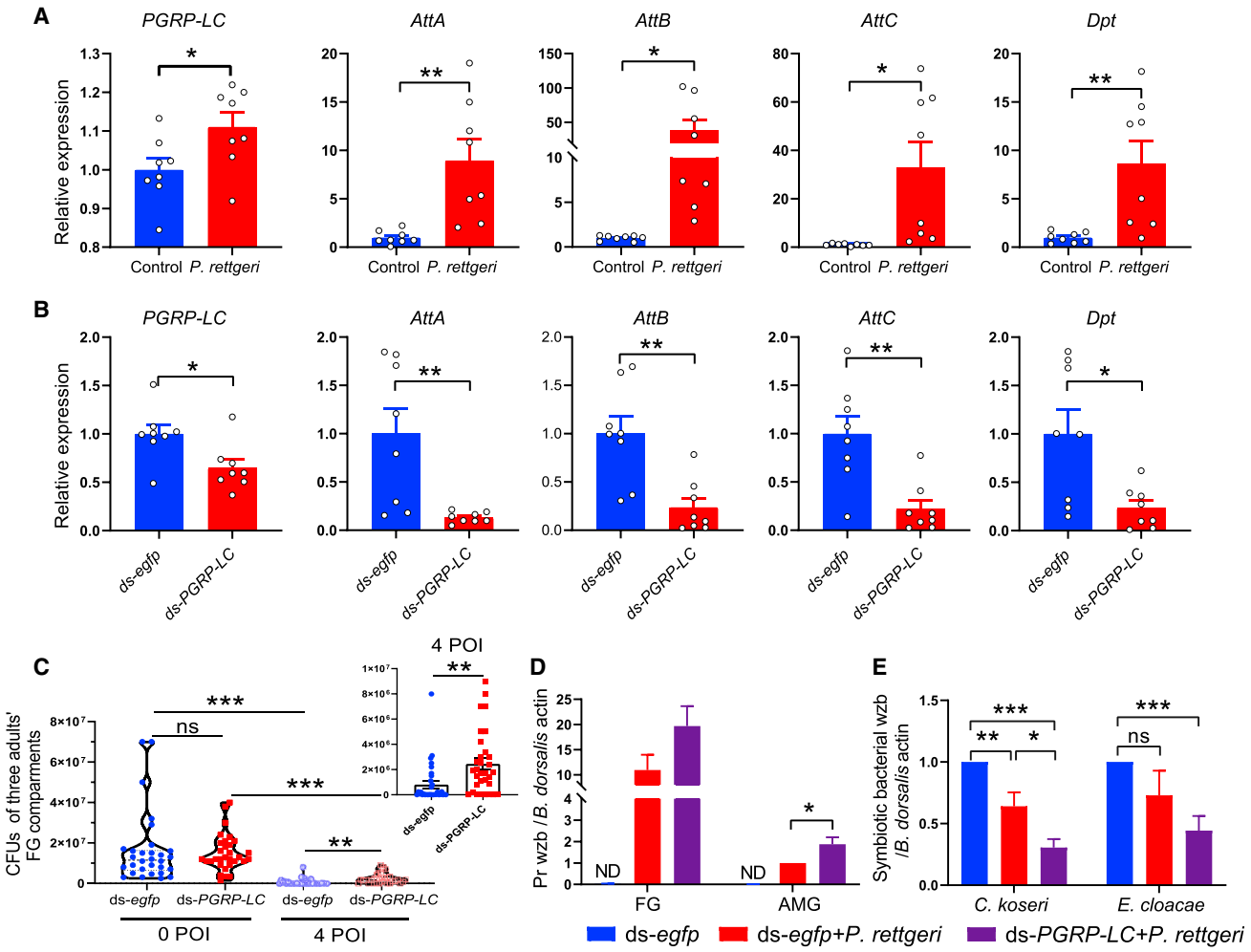

Figure 5. *PGRP-LC* and *AMPs* in the foregut protect symbiotic bacteria from suppression induced by *P. rettgeri*

(A) qPCR analysis of *PGRP-LC* and *AMP* (*AttA*, *AttB*, *AttC*, and *Dpt*) expression in the FG region after oral infection with *P. rettgeri*. FG samples were collected at 9 h post *P. rettgeri* infection; 5% sucrose water was administered as a vehicle control. Values were normalized to *Rpl32* expression (n = 8).

(B) qPCR analysis of *PGRP-LC* and *AMP* (*AttA*, *AttB*, *AttC*, and *Dpt*) expression in the FG region after knockdown of *PGRP-LC*. FG samples were collected before feeding *P. rettgeri* to ds-*egfp*- or ds-*PGRP-LC* treated flies. Values were normalized to *Rpl32* expression (n = 8).

(C) Colony forming units in FG from *ds-egfp*-treated flies (blue circles), and flies with knockdown of *PGRP-LC* (red squares), orally infected with *P. rettgeri*. Serial dilutions were prepared from foregut extracts and plated at 0 and 4 h post oral infection (POI) with *P. rettgeri*. After 0 h POI, the remaining flies were not fed anything (n = 30–32).

(D) The density of *P. rettgeri* was detected by qPCR in the FG and AMG at 12 h POI by qPCR. Values were normalized to β-*actin* expression (n = 13).

(E) The density of symbiotic bacteria *C. koseri* and *E. cloacae* was measured in the AMG at 12 h POI by qPCR. Values were normalized to β-actin expression (n = 10 for *C. koseri* and n = 11 for *E. cloacae*). Data represent mean ± SEM for biological replicates, *p < 0.05, **p < 0.01, ***p < 0.001 with a two-tailed Student's t test, ND, not detected; ns, not significant (p > 0.05). See also Figure S4.

Providencia rettgeri, and monitored the expression of *PGRP-LC* and *AMP* genes by qPCR. We found that oral infection with *P. rettgeri* significantly increased expression of *PGRP-LC*, *AttA*, *AttB*, *AttC*, and *Dpt* in the foregut compared with uninfected flies (Figure 5A). In contrast, oral infection with *P. rettgeri* did not significantly induce the expression of *AMPs* in the AMG region, although *AttC* was modestly induced (Figures S4A–S4D). Monitoring *P. rettgeri* abundance in the gut from 0 to 72 h post oral infection (POI) revealed that *P. rettgeri* accumulated in the foregut, while only small numbers were detected in the AMG region at 0–12 h POI (Figure S4E). We found that *P. rettgeri* density decreased in both the foregut and AMG region over time, and finally became undetectable in the foregut at 48 h POI (Figure S4E). To further characterize the role of the Imd pathway in defense against *P. rettgeri*, we silenced *PGRP-LC* by injecting ds-*PGRP-LC*. This treatment effectively reduced the expression of *PGRP-LC* and *AMPs* in the foregut (Figure 5B). The reduced Imd immune response in the foregut of ds-*PGRP-LC*-treated flies resulted in significantly higher *P. rettgeri* loads at 4 h POI compared with control ds-*egfp*-treated flies (Figure 5C). Due to another immune pathway, the Duox-ROS system that also plays a vital role in the control of pathogens in the gut

(Lee et al., 2013; Yao et al., 2016), we silenced *PGPR-LC* and *Duox* separately or simultaneously (Figures S4F–S4H). Interestingly, *P. rettgeri* loads in the mix of ds-*PGRP-LC*- and ds-*Duox*-treated flies increased significantly when compared with control ds-*egfp*-treated flies at 4 h POI (Figure S4H), or flies singly treated with ds-*PGRP-LC* or ds-*Duox* (Figure S4H). The compensatory upregulation of *Duox* in the foregut upon *PGRP-LC* knockdown explains the much stronger phenotype with the combined knockdown of *PGRP-LC* and *Duox* (Figure S4G). These results indicate that the Imd pathway plays a critical role in controlling bacteria in the foregut, but its activity is partially covered by the activity of the Duox-ROS system.

Activation of the Imd pathway in the foregut protects against dysbiosis of symbiotic bacteria induced by *P. rettgeri*

We next hypothesized that Imd pathway activation in the foregut could be critical to protect the gut microbiota in the AMG by limiting colonization by invading pathogens. We analyzed gut microbiota composition in the AMG of flies with reduced *PGRP-LC* subjected to *P. rettgeri* oral infection. Interestingly, suppressing the Imd immune response in the foregut by silencing *PGRP-LC* resulted in significantly higher *P. rettgeri* abundance not only in the foregut but also in the AMG region compared with controls (Figure 5D). Strikingly, silencing *PGRP-LC* in flies orally infected with *P. rettgeri* led to significant reductions in the abundance of the symbiotic bacteria *C. koseri* and *E. cloacae* in the AMG compared with ds-*egfp* controls (Figure 5E). We conclude that the Imd pathway plays a major role in the defense against invading pathogenic bacteria while protecting symbiotic bacteria in the AMG. As *PGRP-LC* gene expression is specifically enriched in the foregut, this suggests that PGRP-LC exerts a protective effect on symbiotic bacteria through its ability to regulate *AMPs* in the foregut and filter the entry of pathogenic bacteria.

DISCUSSION

The gastrointestinal tract harbors a great diversity of symbiotic bacteria that influence many aspects of the host (Engel and Moran, 2013). The long-term evolutionary interaction of the host immune system with symbiotic bacteria determines their cooperative rather than antagonistic relationship (Pang et al., 2016). How the host tolerates the presence of gut-colonizing autochthonous symbiotic bacteria while responding to and eliminating potential pathogens remains a major enigma in mucosal immunity. The metazoan gastrointestinal tract is a complex tissue composed of multiple compartments bearing different immune components, pH, and oxygen levels (Broderick et al., 2014; Buchon et al., 2013a; Ceja-Navarro et al., 2014; Donaldson et al., 2016; Marianes and Spradling, 2013; Neyen et al., 2012; Zheng et al., 2017) that perform different functions (Geng et al., 2018; Hudry et al., 2019). In this study, we mapped the localization of the bacterial community in different gut regions of *B. dorsalis*, and found that the distribution of symbiotic Enterobacteriaceae bacteria, such as *Citrobacter* and *Enterobacter*, etc. were concentrated in the anterior midgut. Gut microbiota compartmentalization also occurs in other insects, such as *Odontotaenius disjunctus*, *Nicrophorus vespilloides*, *Anabrus simplex*, *Apis mellifera*, and *Drosophila melanogaster* (Broderick et al., 2014; Ceja-Navarro et al., 2014; Li et al., 2016; Martinson et al., 2012; Smith et al., 2017; Vogel et al., 2017), and in mammals, including humans, macaques, mice, cows, and flying squirrels (Donaldson et al., 2016). In *Drosophila*, the acidic copper cell region (CCR) in the middle midgut controls the distribution and the composition of the microbiota. The AMG-located commensal bacterium *Lactobacillus plantarum* appears to colonize the PMG of flies after disruption of the CCR (Li et al., 2016). *L. plantarum* overgrowth in the gut of flies mutant for the immune regulator *PGRP-SD* leads to precocious intestinal aging and a shortened lifespan (Iatsenko et al., 2018). On the whole, maintaining the compartmentalization homeostasis of gut microbiota is critical for animal health.

Previous studies have highlighted the role of amidase PGRPs as negative regulators of the Imd pathway in the gut (Charroux et al., 2018; Paredes et al., 2011). Despite the established importance of the Imd pathway in the gut, little is known about mechanisms by which Imd signaling tolerates symbiotic microbiota while combatting pathogens. Due to the transience of gut microbiota in laboratory populations of *Drosophila* (Broderick et al., 2014; Storelli et al., 2018), it is a poor model in which to study stable colonization of the host, and correspondence between microbiota and host gene expression. In contrast, the gut of *B. dorsalis* harbors a stable and abundant microbiota (Cai et al., 2018; Wang et al., 2011; Yao et al., 2016), which has allowed characterization of the microbiota tolerance mechanism. Our study reveals that Imd pathway activation in the digestive tract of this insect is highly compartmentalized. Strong Imd pathway activity associated with high *PGRP-LC* and *AMP* gene expression is observed in foregut and hindgut but not the midgut. In contrast, the negative regulators *PGRP-LB*, *PGRP-SB*, and *PGRP-SC2* were highly expressed in the midgut. Moreover, our data show that high expression of negative regulators keep the Imd pathway in check in the midgut. Our study shows that the low Imd activity in the AMG establishes a niche that favors cultivation of beneficial microbiota. Simultaneous knockdown of *PGRP-LB* and *PGRP-SB* induced overexpression of *AMPs* in gut, leading to a significant reduction in symbiotic Enterobacteriaceae bacteria, and to a significant increase of the opportunistic pathogens *Providencia* and *Morganella*. Our data are consistent with a previous study showing that high expression of antimicrobial peptides in *Caudal* RNAi flies favors growth of the pathobiont *Gluconobacter* in the gut of *Drosophila*, which is more resistant to antibacterial peptides (Ryu et al., 2008). We further found that the disrupted gut microbiota returned to normal as the RNAi effects dissipated and *PGRP-LB* and *PGRP-SB* returned to basal expression levels. This indicates that the gut microbiota of *B. dorsalis* is resilient to perturbation. Similarly, the composition of the bacterial flora of PGRP-deficient mice is significantly altered, and PGRPs can prevent aberrant inflammatory responses by promoting normal bacterial flora (Saha et al., 2010). Collectively these studies point to a conserved role of PGRPs as modulators of host-microbe interactions in the gut. Our study in *B. dorsalis* shows that two amidase PGRPs, *PGRP-LB* and *PGRP-SB,* reduce intestinal immune reactivity in the AMG, while another PGRP, *PGRP-SC2,* is

expressed in the posterior midgut. *PGRP-LB* and *PGRP-SB* are active only on DAP-type peptidoglycan found in gram-negative bacteria and *Bacillus* (Mellroth and Steiner, 2006; Zaidman-Rémy et al., 2006, 2011), while *PGRP-SC2* has a broader activity range targeting both DAP and Lysine type peptidoglycan (Mellroth et al., 2003). Thus, the specific expression profile of various PGRPs with different enzymatic activities could shape the microbiota along the gut. In addition, we found that gut microbiota homeostasis was not affected by silencing *PGRP-LB* or *PGRP-SB* individually. This suggests a certain level of redundancy and that both genes are needed to scavenge peptidoglycans and prevent expression of diverse *AMPs* that suppress beneficial gut microbes. Collectively, our results demonstrate that a combined action of *PGRP-LB* and *PGRP-SB* in the AMG provides a suitable low-AMP environment for symbiotic Enterobacteriaceae to persist in this gut compartment.

That expression of amidase PGRPs dampens the immune system to favor beneficial bacteria in the gut creates a conundrum, as this could reduce the ability of the insect to fight opportunistic pathogens that enter through the oral route. Our study reveals that compartmentalization of the immune system along the gut provides a solution by mounting a potent immune response in the foregut, without affecting symbiotic bacteria. Indeed, our study shows that *PGRP-LC* and *AMP* genes are expressed at higher level in the foregut and their expression is markedly increased upon oral infection with the opportunistic pathogen *P. rettgeri*. Silencing *PGRP-LC* led to the invasion of *P. rettgeri* not only in the foregut but also in the AMG region. As *PGRP-LC* is mostly expressed in the foregut, we assume this is primarily due to reduction of *PGRP-LC* in the foregut. Interestingly, disruption of *PGRP-LC* not only affects *P. rettgeri,* but also disrupts the microbiota, as illustrated by a reduction in the abundance of the symbiotic *C. koseri* and *E. cloacae*. Thus, our study reveals a prominent role of the foregut in host defense against invading pathogens in filtering incoming bacteria, while the midgut immune system is specialized to maintain beneficial bacteria. It is worth noting that the regulation of the immune response in the foregut does not only involve the Imd pathway but also the production of ROS by NADPH, lysozyme production, and likely other mechanisms, that require further investigation (Ryu et al., 2008; Lee et al., 2013; Yao et al., 2016; Marra et al., 2021).

These results led us to propose a model in which the Imd pathway balances mucosal immunity and regionalized gut-microbe homeostasis. Symbiotic bacteria are mainly located in anterior midgut of *B. dorsalis*; their distribution perfectly matches the expression pattern of amidase PGRPs, indicating that *PGRP-LB* and *PGRP-SB* establish a protective zone by dampening Imd pathway activation. In contrast, the expression of *PGRP-LC* and the absence of *PGRP-LB/SB* in the foregut maintains a higher level of basal and inducible *AMP* expression to protect from potential invading pathogens, effectively avoiding disruption of symbiotic bacteria. Given the universality of symbiotic bacteria compartmentalization in the gut (Donaldson et al., 2016), and dysbiosis of intestinal microbiota that arises from abnormal immune-microbe interactions (Chen et al., 2019; Iatsenko et al., 2018), our results may be of significance to other metazoans, including vertebrates.

Limitations of the study

One limitation of our study is that it relies on the use of systemic injection of dsRNA for gene silencing. This method leads to a systemic knockdown of gene expression affecting all the tissues. However, our model provides the most parsimonious explanation by suggesting that the effects we observed are due to their impact on gene expressed in the gut, where these genes are enriched. Another limitation of our study is that the mechanisms we discovered that allow to construct a protective zone for symbiotic microbiota while maintaining the ability to fight pathogens could be restricted to *B. dorsalis*. Future research is needed to determine if similar mechanisms also exist in other insects, because other factors, such as food digestion, different pH and oxygen gradient along the intestine, and peristalsis are likely also influencing the regional distribution and composition of microbiome along the gut besides the regionalized Imd pathway expression.

STAR★METHODS

Detailed methods are provided in the online version of this paper and include the following:

- KEY RESOURCES TABLE
- RESOURCE AVAILABILITY
  - Lead contact
  - Materials availability
  - Data and code availability
- EXPERIMENTAL MODEL AND SUBJECT DETAILS
  - Insect rearing
- METHOD DETAILS
  - Antibiotic treatment
  - Gut dissection
  - Determinate pH in the gut lumen of *B. dorsalis*
  - RNA extraction and sequencing
  - Differential gene expression analysis
  - Bacterial DNA extraction and 16S rDNA amplicon sequencing
  - Gut bacterial cultures, quantification and identification
  - Microbial oral infection
  - Quantification of bacterial species or group by qPCR
  - Gene expression analysis by qPCR
  - dsRNA synthesis and RNAi experiments
  - Gut tissue sections and RNA FISH
- QUANTIFICATION AND STATISTICAL ANALYSIS

SUPPLEMENTAL INFORMATION

Supplemental information can be found online at https://doi.org/10.1016/j.celrep.2022.111523.

ACKNOWLEDGMENTS

This work was supported by the National Natural Science Foundation of China (no. 31872931, 31801744, and 31572008), the earmarked fund for CARS (no. CARS-26). We thank Prof. Marcelo Jacobs-Lorena (Johns Hopkins University, USA), Dr. Michael Ben-Yosef (Department of Entomology, Agricultural Research Organization, Gilat Center, Israel), Prof. Xiaoxue Li (Huazhong Agricultural University, China), and Hannah Westlake (EPFL, Lausanne,

Switzerland) for correct English usage and their insightful advice and comments that improved the manuscript.

AUTHOR CONTRIBUTIONS

H.Z. and Z.Y. conceived and designed the project. Z.Y. performed experiments and analyzed data. Z.Y., Z.C., and Q.M. made the graphs. Q.M., S.B., Y.W., P.Z., Q.G., and J.G. reared the flies, did the antibiotic treated experiments, and counted the number of CFUs of cultural bacteria. H.Z., Z.Y., and B.L. wrote the manuscript. All authors read and approved the final manuscript.

DECLARATION OF INTERESTS

The authors declare no competing interests.

Received: March 16, 2022
Revised: May 18, 2022
Accepted: September 27, 2022
Published: October 18, 2022

REFERENCES

Bartosch, S., Fite, A., Macfarlane, G.T., and McMurdo, M.E.T. (2004). Characterization of bacterial communities in feces from healthy elderly volunteers and hospitalized elderly patients by using real-time PCR and effects of antibiotic treatment on the fecal microbiota. Appl. Environ. Microbiol. *70*, 3575–3581. https://doi.org/10.1128/AEM.70.6.3575-3581.2004.

Bischoff, V., Vignal, C., Duvic, B., Boneca, I.G., Hoffmann, J.A., and Royet, J. (2006). Downregulation of the *Drosophila* immune response by peptidoglycan recognition proteins SC1 and SC2. PLoS Pathog. *2*, e14. https://doi.org/10.1371/journal.ppat.0020014.

Bosco-Drayon, V., Poidevin, M., Boneca, I.G., Narbonne-Reveau, K., Royet, J., and Charroux, B. (2012). Peptidoglycan sensing by the receptor PGRP-LE in the *Drosophila* gut induces immune responses to infectious bacteria and tolerance to microbiota. Cell Host Microbe *12*, 153–165. https://doi.org/10.1016/j.chom.2012.06.002.

Bruno, D., Bonelli, M., De Filippis, F., Di Lelio, I., Tettamanti, G., Casartelli, M., Ercolini, D., and Caccia, S. (2018). The intestinal microbiota of *Hermetia illucens* larvae is affected by diet and shows a diverse composition in the different midgut regions. Appl. Environ. Microbiol. *85*, 018644-18–18. https://doi.org/10.1128/AEM.01864-18.

Broderick, N.A., Buchon, N., and Lemaitre, B. (2014). Microbiota-induced changes in *Drosophila melanogaster* host gene expression and gut morphology. mBio *5*, e011177-14. https://doi.org/10.1128/mBio.01117-14.

Buchon, N., Broderick, N.A., and Lemaitre, B. (2013b). Gut homeostasis in a microbial world: insights from *Drosophila melanogaster*. Nat. Rev. Microbiol. *11*, 615–626. https://doi.org/10.1038/nrmicro3074.

Buchon, N., Osman, D., David, F.P.A., Fang, H.Y., Boquete, J.P., Deplancke, B., and Lemaitre, B. (2013a). Morphological and molecular characterization of adult midgut compartmentalization in *Drosophila*. Cell Rep. *3*, 1725–1738. https://doi.org/10.1016/j.celrep.2013.04.001.

Carboni, A.L., Hanson, M.A., Lindsay, S.A., Wasserman, S.A., and Lemaitre, B. (2022). Cecropins contribute to *Drosophila* host defense against a subset of fungal and Gram-negative bacterial infection. Genetics *220*, iyab188. https://doi.org/10.1093/genetics/iyab188.

Cai, Z., Yao, Z., Li, Y., Xi, Z., Bourtzis, K., Zhao, Z., Bai, S., and Zhang, H. (2018). Intestinal probiotics restore the ecological fitness decline of *Bactrocera dorsalis* by irradiation. Evol. Appl. *11*, 1946–1963. https://doi.org/10.1111/eva.12698.

Ceja-Navarro, J.A., Nguyen, N.H., Karaoz, U., Gross, S.R., Herman, D.J., Andersen, G.L., Bruns, T.D., Pett-Ridge, J., Blackwell, M., and Brodie, E.L. (2014). Compartmentalized microbial composition, oxygen gradients and nitrogen fixation in the gut of *Odontotaenius disjunctus*. ISME J. *8*, 6–18. https://doi.org/10.1038/ismej.2013.134.

Ceja-Navarro, J.A., Vega, F.E., Karaoz, U., Hao, Z., Jenkins, S., Lim, H.C., Kosina, P., Infante, F., Northen, T.R., and Brodie, E.L. (2015). Gut microbiota mediate caffeine detoxification in the primary insect pest of coffee. Nat. Commun. *6*, 7618. https://doi.org/10.1038/ncomms8618.

Charroux, B., Capo, F., Kurz, C.L., Peslier, S., Chaduli, D., Viallat-Lieutaud, A., and Royet, J. (2018). Cytosolic and secreted peptidoglycan-degrading enzymes in *Drosophila* respectively control local and systemic immune responses to microbiota. Cell Host Microbe *23*, 215–228.e4. https://doi.org/10.1016/j.chom.2017.12.007.

Chen, K., Luan, X., Liu, Q., Wang, J., Chang, X., Snijders, A.M., Mao, J.H., Secombe, J., Dan, Z., Chen, J.H., et al. (2019). *Drosophila* histone demethylase KDM5 regulates social behavior through immune control and gut microbiota maintenance. Cell Host Microbe *25*, 537–552.e8. https://doi.org/10.1016/j.chom.2019.02.003.

Chen, S.L., Dai, S.M., Lu, K.H., and Chang, C. (2008). Female-specific doublesex dsRNA interrupts yolk protein gene expression and reproductive ability in oriental fruit fly, *Bactrocera dorsalis* (Hendel). Insect Biochem. Mol. Biol. *38*, 155–165. https://doi.org/10.1016/j.ibmb.2007.10.003.

Cheng, D., Guo, Z., Riegler, M., Xi, Z., Liang, G., and Xu, Y. (2017). Gut symbiont enhances insecticide resistance in a significant pest, the oriental fruit fly *Bactrocera dorsalis* (Hendel). Microbiome *5*, 13. https://doi.org/10.1186/s40168-017-0236-z.

Clarke, A.R., Armstrong, K.F., Carmichael, A.E., Milne, J.R., Raghu, S., Roderick, G.K., and Yeates, D.K. (2005). Invasive phytophagous pests arising through a recent tropical evolutionary radiation: the *Bactrocera dorsalis* complex of fruit flies. Annu. Rev. Entomol. *50*, 293–319. https://doi.org/10.1146/annurev.ento.50.071803.130428.

Clark, R.I., Salazar, A., Yamada, R., Fitz-Gibbon, S., Morselli, M., Alcaraz, J., Rana, A., Rera, M., Pellegrini, M., Ja, W.W., and Walker, D.W. (2015). Distinct shifts in microbiota composition during *Drosophila* aging impair intestinal function and drive mortality. Cell Rep. *12*, 1656–1667. https://doi.org/10.1016/j.celrep.2015.08.004.

Davidson, N.M., and Oshlack, A. (2014). Corset: enabling differential gene expression analysis for de novo assembled transcriptomes. Genome Biol. *15*, 410. https://doi.org/10.1186/s13059-014-0410-6.

Dillon, R.J., and Dillon, V.M. (2004). The gut bacteria of insects: nonpathogenic interactions. Annu. Rev. Entomol. *49*, 71–92. https://doi.org/10.1146/annurev.ento.49.061802.123416.

Donaldson, G.P., Lee, S.M., and Mazmanian, S.K. (2016). Gut biogeography of the bacterial microbiota. Nat. Rev. Microbiol. *14*, 20–32. https://doi.org/10.1038/nrmicro3552.

Endt, K., Stecher, B., Chaffron, S., Slack, E., Tchitchek, N., Benecke, A., Van Maele, L., Sirard, J.C., Mueller, A.J., Heikenwalder, M., et al. (2010). The microbiota mediates pathogen clearance from the gut lumen after non-typhoidal *Salmonella* diarrhea. PLoS Pathog. *6*, e1001097. https://doi.org/10.1371/journal.ppat.1001097.

Engel, P., and Moran, N.A. (2013). The gut microbiota of insects-diversity in structure and function. FEMS Microbiol. Rev. *37*, 699–735. https://doi.org/10.1111/1574-6976.12025.

Geng, A., Cheng, Y., Wang, Y., Zhu, D., Le, Y., Wu, J., Xie, R., Yuan, J.S., and Sun, J. (2018). Transcriptome analysis of the digestive system of a wood-feeding termite (*Coptotermes formosanus*) revealed a unique mechanism for effective biomass degradation. Biotechnol. Biofuels *11*, 24. https://doi.org/10.1186/s13068-018-1015-1.

Grabherr, M.G., Haas, B.J., Yassour, M., Levin, J.Z., Thompson, D.A., Amit, I., Adiconis, X., Fan, L., Raychowdhury, R., Zeng, Q., et al. (2011). Full-length transcriptome assembly from RNA-Seq data without a reference genome. Nat. Biotechnol. *29*, 644–652. https://doi.org/10.1038/nbt.1883.

Guo, L., Karpac, J., Tran, S.L., and Jasper, H. (2013). PGRP-SC2 promotes gut immune homeostasis to limit commensal dysbiosis and extend lifespan. Cell *156*, 109–122. https://doi.org/10.1016/j.cell.2013.12.018.

Guo, Q., Yao, Z., Cai, Z., Bai, S., and Zhang, H. (2022). Gut fungal community and its probiotic effect on *Bactrocera dorsalis*. Insect Sci. *29*, 1145–1158. https://doi.org/10.1111/1744-7917.12986.

Hanson, M.A., Dostálová, A., Ceroni, C., Poidevin, M., Kondo, S., and Lemaitre, B. (2019). Synergy and remarkable specificity of antimicrobial peptides in vivo using a systematic knockout approach. Elife *8*, e44341. https://doi.org/10.7554/eLife.44341.

Hedengren-Olcott, M., Olcott, M.C., Mooney, D.T., Ekengren, S., Geller, B.L., and Taylor, B.J. (2004). Differential activation of the NF-kappaB-like factors Relish and Dif in *Drosophila melanogaster* by fungi and Gram-positive bacteria. J. Biol. Chem. *279*, 21121–21127. https://doi.org/10.1074/jbc.M313856200.

Huang, H., Li, H., Ren, L., and Cheng, D. (2019). Microbial communities in different developmental stages of the oriental fruit fly, *Bactrocera dorsalis*, are associated with differentially expressed peptidoglycan recognition protein-encoding genes. Appl. Environ. Microbiol. *85*, e00803-19–e00819. https://doi.org/10.1128/AEM.00803-19.

Hudry, B., de Goeij, E., Mineo, A., Gaspar, P., Hadjieconomou, D., Studd, C., Mokochinski, J.B., Kramer, H.B., Plaçais, P.Y., Preat, T., and Miguel-Aliaga, I. (2019). Sex differences in intestinal carbohydrate metabolism promote food intake and sperm maturation. Cell *178*, 901–918.e16. https://doi.org/10.1016/j.cell.2019.07.029.

Iatsenko, I., Boquete, J.P., and Lemaitre, B. (2018). Microbiota-derived lactate activates production of reactive oxygen species by the intestinal NADPH oxidase Nox and shortens *Drosophila* lifespan. Immunity *49*, 929–942.e5. https://doi.org/10.1016/j.immuni.2018.09.017.

Pais, I.S., Valente, R.S., Sporniak, M., and Teixeira, L. (2018). *Drosophila melanogaster* establishes a species-specific mutualistic interaction with stable gut-colonizing bacteria. PLoS Biol. *16*, e2005710. https://doi.org/10.1371/journal.pbio.2005710.

Lee, K.A., Kim, S.H., Kim, E.K., Ha, E.M., You, H., Kim, B., Kim, M.J., Kwon, Y., Ryu, J.H., and Lee, W.J. (2013). Bacterial-derived uracil as a modulator of mucosal immunity and gut-microbe homeostasis in. Cell *153*, 797–811. https://doi.org/10.1016/j.cell.2013.04.009.

Lemaitre, B., and Hoffmann, J. (2007). The host defense of *Drosophila melanogaster*. Annu. Rev. Immunol. *25*, 697–743. https://doi.org/10.1146/annurev.immunol.25.022106.141615.

Li, B., and Dewey, C.N. (2011). RSEM: accurate transcript quantification from RNA-Seq data with or without a reference genome. BMC Bioinf. *12*, 323. https://doi.org/10.1186/1471-2105-12-323.

Li, H., Qi, Y., and Jasper, H. (2016). Preventing age-related decline of gut compartmentalization limits microbiota dysbiosis and extends lifespan. Cell Host Microbe *19*, 240–253. https://doi.org/10.1016/j.chom.2016.01.008.

Li, H., Ren, L., Xie, M., Gao, Y., He, M., Hassan, B., Lu, Y., and Cheng, D. (2020). Egg-surface bacteria are indirectly associated with oviposition aversion in *Bactrocera dorsalis*. Curr. Biol. *30*, 4432–4440.e4. https://doi.org/10.1016/j.cub.2020.08.080.

Li, X., Zhang, M., and Zhang, H. (2011). RNA interference of four genes in adult *Bactrocera dorsalis* by feeding their dsRNAs. PLoS One *6*, e17788. https://doi.org/10.1371/journal.pone.0017788.

Liehl, P., Blight, M., Vodovar, N., Boccard, F., and Lemaitre, B. (2006). Prevalence of local immune response against oral infection in a *Drosophila/Pseudomonas* infection model. PLoS Pathog. *2*, e56. https://doi.org/10.1371/journal.ppat.0020056.

Livak, K.J., and Schmittgen, T.D. (2001). Analysis of relative gene expression data using real-time quantitative PCR and the 2(-Delta Delta C(T)) Method. Methods *25*, 402–408. https://doi.org/10.1006/meth.2001.1262.

Marianes, A., and Spradling, A.C. (2013). Physiological and stem cell compartmentalization within the *Drosophila* midgut. Elife *2*, e00886. https://doi.org/10.7554/eLife.00886.

Marra, A., Hanson, M.A., Kondo, S., Erkosar, B., and Lemaitre, B. (2021). *Drosophila* antimicrobial peptides and lysozymes regulate gut microbiota composition and abundance. mBio *12*, e0082421. https://doi.org/10.1128/mBio.00824-21.

Martin, M. (2011). Cutadapt removes adapter sequences from high-throughput sequencing reads. EMBnet. j. *17*, 10–12. https://doi.org/10.1089/cmb.2017.0096.

Martinson, V.G., Moy, J., and Moran, N.A. (2012). Establishment of characteristic gut bacteria during development of the honeybee worker. Appl. Environ. Microbiol. *78*, 2830–2840. https://doi.org/10.1128/AEM.07810-11.

Matsuda, K., Tsuji, H., Asahara, T., Matsumoto, K., Takada, T., and Nomoto, K. (2009). Establishment of an analytical system for the human fecal microbiota, based on reverse transcription-quantitative PCR targeting of multicopy rRNA molecules. Appl. Environ. Microbiol. *75*, 1961–1969. https://doi.org/10.1128/AEM.01843-08.

Mellroth, P., Karlsson, J., and Steiner, H. (2003). A scavenger function for a *Drosophila* peptidoglycan recognition protein. J. Biol. Chem. *278*, 7059–7064. https://doi.org/10.1074/jbc.M208900200.

Mellroth, P., and Steiner, H. (2006). PGRP-SB_1: an N-acetylmuramoyl L-alanine amidase with antibacterial activity. Biochem. Biophys. Res. Commun. *350*, 994–999. https://doi.org/10.1016/j.bbrc.2006.09.139.

Moter, A., and Göbel, U.B. (2000). Fluorescence in situ hybridization (FISH) for direct visualization of microorganisms. J. Microbiol. Methods *41*, 85–112. https://doi.org/10.1016/s0167-7012(00)00152-4.

Neyen, C., Poidevin, M., Roussel, A., and Lemaitre, B. (2012). Tissue- and ligand-specific sensing of gram-negative infection in *Drosophila* by PGRP-LC isoforms and PGRP-LE. J. Immunol. *189*, 1886–1897. https://doi.org/10.4049/jimmunol.1201022.

Nyholm, S.V., and Graf, J. (2012). Knowing your friends: invertebrate innate immunity fosters beneficial bacterial symbioses. Nat. Rev. Microbiol. *10*, 815–827. https://doi.org/10.1038/nrmicro2894.

Pan, X., Zhou, G., Wu, J., Bian, G., Lu, P., Raikhel, A.S., and Xi, Z. (2012). Wolbachia induces reactive oxygen species (ROS)-dependent activation of the Toll pathway to control dengue virus in the mosquito *Aedes aegypti*. Proc. Natl. Acad. Sci. USA *109*, E23–E31. https://doi.org/10.1073/pnas.1116932108.

Pang, X., Xiao, X., Liu, Y., Zhang, R., Liu, J., Liu, Q., Wang, P., and Cheng, G. (2016). Mosquito C-type lectins maintain gut microbiome homeostasis. Nat. Microbiol. *1*, 16023. https://doi.org/10.1038/nmicrobiol.2016.23.

Paredes, J.C., Welchman, D.P., Poidevin, M., and Lemaitre, B. (2011). Negative regulation by amidase PGRPs shapes the *Drosophila* antibacterial response and protects the fly from innocuous infection. Immunity *35*, 770–779. https://doi.org/10.1016/j.immuni.2011.09.018.

Raza, M.F., Wang, Y., Cai, Z., Bai, S., Yao, Z., Awan, U.A., Zhang, Z., Zheng, W., and Zhang, H. (2020). Gut microbiota promotes host resistance to low-temperature stress by stimulating its arginine and proline metabolism pathway in adult *Bactrocera dorsalis*. PLoS Pathog. *16*, e1008441. https://doi.org/10.1371/journal.ppat.1008441.

Ren, L., Ma, Y., Xie, M., Lu, Y., and Cheng, D. (2021). Rectal bacteria produce sex pheromones in the male oriental fruit fly. Curr. Biol. *31*, 2220–2226.e4. https://doi.org/10.1016/j.cub.2021.02.046.

Round, J.L., and Mazmanian, S.K. (2009). The gut microbiota shapes intestinal immune responses during health and disease. Nat. Rev. Immunol. *9*, 313–323. https://doi.org/10.1038/nri2515.

Ryu, J.H., Kim, S.H., Lee, H.Y., Bai, J.Y., Nam, Y.D., Bae, J.W., Lee, D.G., Shin, S.C., Ha, E.M., and Lee, W.J. (2008). Innate immune homeostasis by the homeobox gene caudal and commensal-gut mutualism in *Drosophila*. Science *319*, 777–782. https://doi.org/10.1126/science.1149357.

Saha, S., Jing, X., Park, S.Y., Wang, S., Li, X., Gupta, D., and Dziarski, R. (2010). Peptidoglycan recognition proteins protect mice from experimental colitis by promoting normal gut flora and preventing induction of interferon-γ. Cell Host Microbe *8*, 147–162. https://doi.org/10.1016/j.chom.2010.07.005.

Shibata, T., Sekihara, S., Fujikawa, T., Miyaji, R., Maki, K., Ishihara, T., Koshiba, T., and Kawabata, S.i. (2013). Transglutaminase-catalyzed protein-protein cross-linking suppresses the activity of the NF-κB-like transcription factor relish. Sci. Signal. *6*, ra61. https://doi.org/10.1126/scisignal.2003970.

Shin, S.C., Kim, S.H., You, H., Kim, B., Kim, A.C., Lee, K.A., Yoon, J.H., Ryu, J.H., and Lee, W.J. (2011). *Drosophila* microbiome modulates host developmental and metabolic homeostasis via insulin signaling. Science *334*, 670–674. https://doi.org/10.1126/science.1212782.

Singh, A.K., and Bhunia, A.K. (2016). Optical scatter patterns facilitate rapid differentiation of Enterobacteriaceae on CHROMagar^{TM} Orientation medium. Microb. Biotechnol. *9*, 127–135. https://doi.org/10.1111/1751-7915.12323.

Smith, C.C., Srygley, R.B., Healy, F., Swaminath, K., and Mueller, U.G. (2017). Spatial structure of the mormon cricket gut microbiome and its predicted contribution to nutrition and immune function. Front. Microbiol. *8*, 801. https://doi.org/10.3389/fmicb.2017.00801.

Stecher, B., and Hardt, W.D. (2011). Mechanisms controlling pathogen colonization of the gut. Curr. Opin. Microbiol. *14*, 82–91. https://doi.org/10.1016/j.mib.2010.10.003.

Storelli, G., Strigini, M., Grenier, T., Bozonnet, L., Schwarzer, M., Daniel, C., Matos, R., and Leulier, F. (2018). *Drosophila* perpetuates nutritional mutualism by promoting the fitness of its intestinal symbiont *Lactobacillus plantarum*. Cell Metabol. *27*, 362–377.e8. https://doi.org/10.1016/j.cmet.2017.11.011.

Tanji, T., Yun, E.Y., and Ip, Y.T. (2010). Heterodimers of NF-kappaB transcription factors DIF and Relish regulate antimicrobial peptide genes in *Drosophila*. Proc. Natl. Acad. Sci. USA *107*, 14715–14720. https://doi.org/10.1073/pnas.1009473107.

Thong-On, A., Suzuki, K., Noda, S., Inoue, J.i., Kajiwara, S., and Ohkuma, M. (2012). Isolation and characterization of anaerobic bacteria for symbiotic recycling of uric acid nitrogen in the gut of various termites. Microb. Environ. *27*, 186–192. https://doi.org/10.1264/jsme2.me11325.

Vogel, H., Shukla, S.P., Engl, T., Weiss, B., Fischer, R., Steiger, S., Heckel, D.G., Kaltenpoth, M., and Vilcinskas, A. (2017). The digestive and defensive basis of carcass utilization by the burying beetle and its microbiota. Nat. Commun. *8*, 15186. https://doi.org/10.1038/ncomms15186.

Wang, H., Jin, L., Peng, T., Zhang, H., Chen, Q., and Hua, Y. (2014). Identification of cultivable bacteria in the intestinal tract of *Bactrocera dorsalis* from three different populations and determination of their attractive potential. Pest Manag. Sci. *70*, 80–87. https://doi.org/10.1002/ps.3528.

Wang, H., Jin, L., and Zhang, H. (2011). Comparison of the diversity of the bacterial communities in the intestinal tract of adult *Bactrocera dorsalis* from three different populations. J. Appl. Microbiol. *110*, 1390–1401. https://doi.org/10.1111/j.1365-2672.2011.05001.x.

Xiao, X., Yang, L., Pang, X., Zhang, R., Zhu, Y., Wang, P., Gao, G., and Cheng, G. (2017). A Mesh-Duox pathway regulates homeostasis in the insect gut. Nat. Microbiol. *2*, 17020. https://doi.org/10.1038/nmicrobiol.2017.20.

Yao, Z., Wang, A., Li, Y., Cai, Z., Lemaitre, B., and Zhang, H. (2016). The dual oxidase gene *BdDuox* regulates the intestinal bacterial community homeostasis of *Bactrocera dorsalis*. ISME J. *10*, 1037–1050. https://doi.org/10.1038/ismej.2015.202.

Zaidman-Rémy, A., Hervé, M., Poidevin, M., Pili-Floury, S., Kim, M.S., Blanot, D., Oh, B.H., Ueda, R., Mengin-Lecreulx, D., and Lemaitre, B. (2006). The *Drosophila* amidase PGRP-LB modulates the immune response to bacterial infection. Immunity *24*, 463–473. https://doi.org/10.1016/j.immuni.2006.02.012.

Zaidman-Rémy, A., Poidevin, M., Hervé, M., Welchman, D.P., Paredes, J.C., Fahlander, C., Steiner, H., Mengin-Lecreulx, D., and Lemaitre, B. (2011). *Drosophila* immunity: analysis of PGRP-SB1 expression, enzymatic activity and function. PLoS One *6*, e17231. https://doi.org/10.1371/journal.pone.0017231.

Zhang, P., Yao, Z., Bai, S., and Zhang, H. (2022). The negative regulative roles of *BdPGRPs* in the Imd signaling pathway of *Bactrocera dorsalis*. Cells *11*, 152. https://doi.org/10.3390/cells11010152.

Zhang, Q., Cai, P., Wang, B., Liu, X., Lin, J., Hua, R., Zhang, H., Yi, C., Song, X., Ji, Q., et al. (2021). Manipulation of gut symbionts for improving the sterile insect technique: quality parameters of *Bactrocera dorsalis* (Diptera: Tephritidae) genetic sexing strain males after feeding on bacteria-enriched diets. J. Econ. Entomol. *114*, 560–570. https://doi.org/10.1093/jee/toaa294.

Zheng, H., Powell, J.E., Steele, M.I., Dietrich, C., and Moran, N.A. (2017). Honeybee gut microbiota promotes host weight gain via bacterial metabolism and hormonal signaling. Proc. Natl. Acad. Sci. USA *114*, 4775–4780. https://doi.org/10.1073/pnas.1701819114.

Zhu, K.Y., and Palli, S.R. (2020). Mechanisms, applications, and challenges of insect RNA interference. Annu. Rev. Entomol. *65*, 293–311. https://doi.org/10.1146/annurev-ento-011019-025224.

STAR★METHODS

KEY RESOURCES TABLE

REAGENT or RESOURCE	SOURCE	IDENTIFIER
Bacterial and virus strains		
Providencia rettgeri V2	This study	N/A
Biological samples		
Bacterial DNA of *B. dorsalis* samples	This study	N/A
RNA of *B. dorsalis* samples	This study	N/A
Chemicals, peptides, and recombinant proteins		
Trizol RNAiso Plus	TaKaRa	Cat# 9109
Critical commercial assays		
PrimeScript™ RT reagent Kit with gDNA Eraser	TaKaRa	Cat# RR047A
E.Z.N.A.® Soil DNA kit	Omega	Cat# D5625-02
T7 Ribomax Express RNAi System	Promega	Cat# P1700
iTaq™ Universal SYBR® Green Supermix	Bio-Rad	Cat# 172-5124
Deposited data		
16S rDNA amplicon sequencing of gut bacteria in *Bactrocera dorsalis*	This study	SRA: PRJNA777066
RNA-seq data for gut regions of *Bactrocera dorsalis*	This study	SRA: PRJNA774500
Oligonucleotides		
Diptericin probe: 5′-TCTATGCC TTGCTTAGGACTACCACCTCCCTGTAA-3′	This study	N/A
See Tables S2 and S3 for the sequences of all the primers	This paper (Bartosch et al., 2004; Li et al., 2011; Matsuda et al., 2009; Yao et al., 2016; Zhang et al., 2022)	N/A
Software and algorithms		
Primer Premier 5.0	Premier Biosoft	http://www.premierbiosoft.com/primerdesign/
GraphPad Prism V8.0	GraphPad Software	https://www.graphpad.com/
SPSS V20.0	IBM	https://www.ibm.com/analytics/spss-statisticssoftware
R statistical software	R Core Team (2021)	https://www.R-project.org/

RESOURCE AVAILABILITY

Lead contact

Further information and requests for resources and reagents should be directed to and will be fulfilled by the lead contact, Hongyu Zhang (hongyu.zhang@mail.hzau.edu.cn).

Materials availability

This study did not generate new, unique reagents.

Data and code availability

- Gut RNA sequencing and Bacterial 16S rDNA amplicon sequencing data have been deposited at SRA Dataset and are publicly available as of the date of publication. Accession numbers are listed in the key resources table.
- This paper does not report original code.
- Any additional information required to reanalyze the data reported in this paper is available from the lead contact upon request.

EXPERIMENTAL MODEL AND SUBJECT DETAILS

Insect rearing

The oriental fruit flies were reared at the Institute of Horticultural and Urban Entomology, Huazhong Agricultural University (Wuhan, China), with a 12 h light/12 h dark cycle at 27 ± 1°C and 70–80% relative humidity. After eclosion, adult flies were moved to 30 × 30 × 30 cm cages and maintained on an artificial diet consisting of 3:1 sucrose/yeast extract. Female flies were used for all experiments.

METHOD DETAILS

Antibiotic treatment

For antibiotic treatment, newly emerged flies were fed on sterile water supplemented with penicillin (3 mg/mL), streptomycin (5 mg/mL), and gentamicin (3 mg/mL), on a cotton pad that was changed every 24 h (Raza et al., 2020).

Gut dissection

Before dissection, flies were surface-sterilized by immersion in 75% ethanol for 3 min and rinsed three times in sterile phosphate-buffered saline (PBS) buffer (pH 7.4) as previously described (Guo et al., 2022). The whole gut was carefully dissected and stretched out in ice-cold PBS with flame-sterilized tools, then cut into five regions for RNA and DNA extraction: (1) foregut-FG, including the pharynx, esophagus, intact crop and cardia; (2) anterior midgut-AMG; (3) middle midgut-MMG; (4) posterior midgut-PMG and (5) hindgut-HG, including the ileum, colon and rectum (Figure 1A).

Determinate pH in the gut lumen of *B. dorsalis*

Two pH indicators-phenol red and bromophenol blue were used to assess the pH values in different gut regions of *B. dorsalis* adult (age: 7 days after emergence). Bromophenol blue is yellow when pH values $\leq$3.0, and blue when pH values $\geq$4.6; phenol red is yellow at pH values $\leq$6.8, and fuchsia at pH values $\geq$8.2, with a gradual color transition for intermediate values as previously described (Bruno et al., 2018). *B. dorsalis* adults were first dehydrated for 24 h without food and then fed an artificial diet (2.5% yeast extract, 7.5% sugar, 2.5% honey and 87% H_2O) supplemented with 0.2% (w/w) bromophenol blue or phenol red for 24 h. Finally, the guts of these flies were carefully dissected and stretched out in ice-cold PBS, and coloration of the gut content was evaluated with a stereomicroscope.

RNA extraction and sequencing

Total RNA was isolated from the five regions of 80 adult guts (age: 7 days after emergence) per biological replicate using RNAiso Plus reagent (Takara, Otsu, Shiga, Japan) according to the manufacturer's instructions, three biological replicates were conducted. RNA degradation was monitored by 1% agarose gel electrophoresis. Total RNA was sent to the Novogene Experimental Department (Tianjin, China) for library preparation and sequencing. The raw sequencing reads were deposited in Short Read Archive at NCBI under the accession number PRJNA774500. Raw reads were first processed through in-house perl scripts to remove reads containing adapter, reads containing poly-N and low quality reads. At the same time, Q20, Q30, GC-content and sequence duplication level of the clean data were calculated. Transcriptome assembly was performed with Trinity (Grabherr et al., 2011) and sequence redundancy was reduced with the sequence clustering tool Corset (Davidson and Oshlack, 2014).

Differential gene expression analysis

Functional gene annotation utilized seven databases: NCBI non-redundant protein sequences (Nr); NCBI non-redundant nucleotide sequences (Nt); Protein family (Pfam); Clusters of Orthologous Groups of proteins (KOG/COG); a manually annotated and reviewed protein sequence database (Swiss-Prot); KEGG Ortholog database (KOG) and Gene Ontology (GO). Gene expression levels were estimated by RNA-Seq by Expectation-Maximization (RSEM) (Li and Dewey, 2011).

Bacterial DNA extraction and 16S rDNA amplicon sequencing

DNA was extracted from 100 gut regions of flies (age: 7 days after emergence) per biological replicate using the E.Z.N.A.® Soil DNA kit (Omega, Norcross, GA, USA) according to the manufacturer's instructions, six biological replicates were conducted. The 16S rRNA gene spanning variable regions V3+V4 was amplified using the broad-range forward primer 341F: CCTAYGGGRBGCASCAG and the reverse primer 806R: GGACTACNNGGGTATCTAAT using the Phusion® High-Fidelity PCR Master Mix (New England Biolabs, Beverley, MA). The PCR amplification program consisted of (1) preincubation at 95°C for 5 min; (2) 35 cycles of 45 s at 56°C, then 1 min at 72°C and 45 s at 94°C; (3) 10 min at 72°C. The PCR products were sent to Novogene Experimental Department for sequencing. The raw sequencing reads were deposited in Short Read Archive at NCBI under the accession number PRJNA777066.

After obtaining the raw reads, the single-end reads were assigned to samples based on their unique barcode and truncated by cutting off the barcode and primer sequence. Quality filtering on the raw reads was performed under specific filtering conditions to obtain high-quality clean reads according to the Cutadapt (b1.9.1, http://cutadapt.readthedocs.io/en/stable/) quality controlled process (Martin, 2011). The reads were compared with the reference database (Silva database, https://www.arb-silva.de/) using

UCHIME algorithm (UCHIME Algorithm, http://www.drive5.com/usearch/manual/uchime_algo.html) to detect chimera sequences, and then the chimera sequences were removed, the Clean Reads finally obtained.

Sequences were clustered into OTUs of ≥97% similarity using Uparse software (Uparse v7.0.1001, http://drive5.com/upare). Representative sequence for each OTU was screened for further annotation, and taxonomy assignment was carried out with mothur algorithm using the silva database. OTUs abundance information were normalized using a standard of sequence number corresponding to the sample with the least sequences. Alpha diversity (including observed-species, chao1, shannon, simpson and ace) and beta diversity on weighted unifrac were calculated with qime and displayed with R software.

Gut bacterial cultures, quantification and identification

Dissected samples of the five gut regions from approximately 30 females (age: 7 days after emergence) were homogenized in 1 mL of sterile phosphate-buffered saline for 60 s using a burnisher at 70hz/s. An aliquot from these samples was serially diluted and plated onto two media: Luria-Bertani (LB) nutrient agar plates and a chromogenic medium CHROMagar™ Orientation (CHR, buy from Shanghai central bio-engineering CO., LTD). After incubation at 30°C for 24–48 h, individual and morphologically distinct colonies counted for colony forming morphologically units (CFUs). LB counts were used for total bacterial CFUs, while CHR can distinguish Enterobacteriaceae strains based on both color and morphology (Singh and Bhunia, 2016); morphological characteristics of different bacterial species in the *B. dorsalis* gut are shown in Figure S5A. To investigate the composition of symbiotic bacteria in different gut regions of *B. dorsalis*, 617 bacterial strains were isolated from CHR medium, then inoculated into corresponding liquid media and shaken at 220 rpm and 30°C overnight to produce biomass for DNA extraction. The bacterial DNA was extracted by using the HiPure Bacterial DNA Kit (Magen, Guangzhou, China). Amplify the 16S rRNA gene by RT-PCR was performed to identify each bacterial isolate, with primers: 27f (5′-GTTTGATCCTGGCTCAG-3′) and 1492r (5′-GGTTACCTTGTTACGACTT-3′) (Ceja-Navarro et al., 2015), under the PCR conditions: 94°C for 3 min; 35 cycles of 94°C for 10 s, 55°C for 10 s, and 72°C for 30 s; 72°C for 5 min. Finally, the PCR products were purified by using E.Z.N.A.® Cycle-Pure kit (Omega, Norcross, GA, USA) and then subjected to bidirectional sanger sequencing. These sequences were BLASTed against the NCBI 16S rRNA sequences database to identify the cultivable bacterial strains.

Microbial oral infection

The opportunistic pathogen *Providencia rettgeri* used for oral infection was grown as a shaking culture in LB medium at 37°C, 220 r.p.m overnight. The culture of ~300 mL was pelleted by centrifugation (5 min at 3,200 g) and adjusted to the appropriate concentration with optical density (O.D.) at 600 nm. Adult flies (age: 3–4 days) were dehydrated for 24 h without food and then fed an artificial diet supplemented with 5% sucrose containing the concentrated microbe solution (*P. rettgeri* OD600= 50). Flies supplemented with 5% sucrose only served as a control. For bacterial count in FG, flies treated with dsRNA were maintained on this diet for 4 h, and subsequently starved. For analyses of Imd pathway immune gene expression and dynamic changes of *P. rettgeri* and symbiotic bacteria in ds-*egfp* or ds-*PGRP-LC* treated flies, they were maintained on this diet for 9 h, and subsequently transferred to fresh food. The gut region samples for different treatments were collected at different time points post oral infection.

Quantification of bacterial species or group by qPCR

Gut bacterial DNA extraction from female flies was performed as described above. For bacteria quantification, real-time quantitative PCR (qPCR) was performed and normalized to the host *β-actin* gene. In this study, *wzb* and *wzc* genes of bacteria were used to design specific qPCR primers for *Citrobacter koseri*, *Enterobacter cloacae*, *Providencia rettgeri* and *Providencia-Morganella* group bacterial density detection; the specificity of qPCR primers was confirmed by RT-PCR (Figures S5B–S5E). RT-PCR was carried out in a volume of 25 μL. Each PCR mixture consisted of 12.5 μL of A8 MasterMix (Aidlab Biotechnologies Co., Ltd), 200 nM of each primer and 100 ng DNA. The amplification program consisted of (1) Initial denaturation 95°C for 3 min; (2) 30 cycles of denaturation at 95°C for 10 s, annealing at 60°C for 15 s and extension at 72°C for 15 s; (3) final extension 72°C for 5 min. All the primers for detection of bacterial groups and species are shown in Table S2. qPCR was carried out in 20 μL reaction volume included 10 μL of SYBR Green Mix (Bio-Rad), 200 nM of each primer and 5 ng of DNA. Real-time PCR was performed using a Bio-Rad CFX Connect system with the following protocol: (1) preincubation at 50°C for 2 min and 95°C for 10 min; (2) 45 cycles of denaturation at 95°C for 15 s and annealing at 60°C for 1 min; and (3) one cycle at 95°C for 15 s, 53°C for 15 s and 95°C for 15 s.

Gene expression analysis by qPCR

For gene expression analysis, five independent cohorts of ~30 flies each were collected for RNA extraction. The first-strand complementary DNA (cDNA) of each pool was synthesized from 1 μg of total RNA using PrimeScript™ RT reagent kit (Takara) with gDNA eraser to remove residual DNA contamination. qPCR was carried out in 20 μL reaction volume included 10 μL of SYBR Green Mix (Bio-Rad), 400 nM of each primer and 2 μL of cDNA (diluted 1:10). Real-time PCR was performed using a Bio-Rad CFX Connect system with the following protocol: initial denaturation of 95°C for 30 s, followed by 45 cycles of 95°C for 15 s and 60°C for 30 s. Melting curve analysis was performed at the end of each amplification run to confirm the presence of a single peak, with the following protocol: 55°C for 60 s, followed by 81 cycles starting at 55°C for 10 s with a 0.5°C increase each cycle. Relative quantification was calculated according to the $2^{-\Delta\Delta Ct}$ method (Livak and Schmittgen, 2001), at least three independent biological replicates and three

technical replicates were performed for every sample. The levels of detected mRNA determined by cycling threshold analysis were normalized using 60S ribosomal protein L32 (*RpL32*) as the control, primers used in qPCR analysis were listed in Table S3.

dsRNA synthesis and RNAi experiments

The RNA interference (RNAi) technique, which generates loss-of-function phenotypes by depletion of a chosen transcript by short/small interfering RNA (siRNA, come from double-stranded RNA cleaved by the enzyme Dicer into ~21 nucleotides), has emerged as a powerful reverse genetics tool for studying gene function, regulation, and interaction at the cellular and organismal levels in many eukaryotic systems, including a number of insect species (Zhu and Palli, 2020). Thanks to the robustness and specificity of RNAi technique, many genes' functions have been revealed in *B. dorsalis* (Chen et al., 2008; Yao et al., 2016; Huang et al., 2019; Raza et al., 2020; Zhang et al., 2022). In this study, specific dsRNA primers with the T7 RNA polymerase promoter (5′-GGATCCTAATACGACTCACTATAGG-3′) on the 5′ end were used to clone the target sequence fragments by nested PCR, sequences of the primers were listed in Table S3. 1 μg PCR product was used as the specific-template for synthesizing of dsRNA *in vitro* by using the T7 Ribomax Express RNAi System (Promega, Madison, WI, USA). The concentration of dsRNA was quantitated at 260 nm using a NanoDrop 2000 Spectrophotometer (Thermo Fisher Scientific Inc.). The quality and integrity of dsRNA were determined by agarose gel electrophoresis. Needles for injecting dsRNA were produced by a puller (PC-10, Narishige, Tokyo, Japan) at heat level 60.8. Microinjection of dsRNA was performed by Eppendorf micromanipulation system (Microinjector for cell biology, FemtoJet 5247, Hamburg, Germany) with Pi of 300 hpa and Ti of 0.3 s as previously described (Yao et al., 2016). RNAi experiments were performed by injecting 1 μL of a 2μg μL^{-1} solution of dsRNA into the ventral abdomen of each fly (2–3 days old). For RNAi of *PGRP-LB* and *PGRP-SB*, or *PGRP-LC* and *Duox* simultaneously, 1 μL of combined ds-*PGRP-LB* + ds-*PGRP-SB*, or ds-*PGRP-LC* + ds-*Duox* dsRNA was injected at the final concentration of 2μg μL^{-1}; control flies were injected with ds-*egfp*.

Gut tissue sections and RNA FISH

Different gut regions of female (age: 7 days after emergence) were carefully dissected in ice-cold PBS and fixed in fixative (including 4% formaldehyde and 0.1M phosphate buffer, pH7.0–7.5) for 2 h at room temperature. After fixation, the tissue was dehydrated by gradient alcohol, dipped into paraffin and embedded. Then paraffin-embedded (FFPE) samples were sectioned to 4 μm thick FFPE tissue sections by a slicer, and FISH staining was performed as previously described (Moter and Gober, 2000). Briefly, FFPE tissue sections were dried under 62°C condition for 2 h, then the tissue sections were sequentially placed into xylene (twice in 30 min), anhydrous ethanol (twice in 10 min), then 85% alcohol (5 min), 75% alcohol (5 min), rinsed with RNAase-free water, lastly boiled in repair solution (15 min). Then added proteinase K (20 μg/mL) for digestion (30 min), and washed three times with PBS. Added pre-hybridization solution and incubated at 37°C for 1 h. Then discarded the pre-hybridization solution and replaced with hybridization solution containing *Dpt* probe (5′-TCTATGCCTTGCTTAGGACTACCACCTCCCTGTAA-3′) overnight at 37°C. The hybridization solution was washed away with 2 × saline sodium citrate (SSC) (10 min), 1 × SSC (twice in 10 min) at 37°C condition, and 0.5 × SSC (10 min) at room temperature. Counterstain by 4′-6-Diamidino-2-phenylindole (DAPI) was performed in the dark condition for 8 min. After washing, antifluorescence quenched sealer was added. DAPI non-specifically stained nuclear nucleic acids and was blue under the ultraviolet laser, while the representative positive signal carboxy-fluorescein (FAM) (488) was green. The images were captured by fluorescence microscope (Nikon Eclipse ci, Japan) with a 100 times magnification.

QUANTIFICATION AND STATISTICAL ANALYSIS

Two-tailed Student's *t*-test were used for two-group comparisons in the GraphPad Prism software. Multiple comparisons were carried out with one-way analysis of variance and Tukey's *post hoc* test using SPSS 20.0 software. The differences were considered statistically significant when a value of $p < 0.05$. Data are represented as mean ± SEM. All statistical details can be found in the according figure legends.